Received: 14 September 2023 | Revised: 27 November 2023 | Accepted: 12 December 2023 | Published online: 24 December 2023

RESEARCH ARTICLE

Journal of Optics and Photonics Research
2024, Vol. 1(2) 51–58
DOI: 10.47852/bonviewJOPR32021730

BON VIEW PUBLISHING

Multimodal Multiphoton Tomography with a Compact Femtosecond Fiber Laser

Karsten König[1,2,*]

[1]*Department of Biophotonics and Laser Technology, Saarland University, Germany*

[2]*JenLab GmbH, Germany*

Abstract: Multiphoton tomography (MPT) based on near infrared (NIR) femtosecond laser technology has become a versatile high-resolution clinical and research imaging tool. We report on multimodal MPT with the air-cooled fiber laser tomograph MPT*compact*. The ultracompact passively mode-locked erbium-doped 50/80 MHz laser operating at 780 nm is directly integrated into the 360° imaging head mounted on a flexible mechanical arm. The tomograph provides optical biopsies with subcellular resolution and optical metabolic imaging capability based on two-photon autofluorescence (AF), second harmonic generation, fluorescence lifetime imaging (FLIM) by time-correlated single photon counting with 250 ps temporal resolution, reflectance confocal microscopy, and white LED light CMOS camera imaging. For the first time, NIR femtosecond laser pulses have been used on human skin to realize simultaneous one-photon confocal imaging and two-photon imaging. Most useful information is provided by the two-photon excited intratissue AF of the coenzymes NAD(P)H and flavins. The signals of both types of coenzymes can be separated by FLIM. Furthermore, the free and protein-bound forms can be distinguished by time-resolved AF detection because the protein-bound NADH has one order higher AF lifetime than free (non-bound) NADH. The tomograph contains onboard storage batteries so that it can operate for up to a few hours independently from external power supply. Applications include in vivo cancer detection and *in situ* evaluation of anti-aging drugs and pharmaceuticals. The tomograph MPT*compact* has been successfully tested in a clinical multicenter study for the diagnosis of malignant melanoma on 100 patients with suspicious pigmented lesions. MPT has the potential to realize non-invasive high-resolution label-free *in vivo* histology within minutes and, therefore, to reduce the number of physically taken biopsies.

Keywords: multiphoton tomography, autofluorescence, SHG, FLIM, reflectance confocal microscopy, two-photon

1. Introduction

Two-photon microscopy was reported by Denk et al. [1]. Seven years later, Masters et al. published the first two-photon excited fluorescence images of human skin [2]. The clinical use of 3D two-photon autofluorescence (AF) imaging and second harmonic generation (SHG) imaging, termed multiphoton tomography (MPT), for label-free *in vivo* evaluation of human skin started in 2003 with the tomograph *DermaInspect* (Figure 1(a)). Fifty-three patients with suspicious pigmented skin lesions had been investigated at the University Jena in Germany. Optical biopsies based on 2108 multiphoton skin sections with intracellular resolution were taken non-invasively without any negative side effects. One year later, the *Certified Body EU0118: Thuringian State Authority of Metrology and Verification (LMET*) approved the multiphoton tomograph *DermaInspect* as first CE-certified medical femtosecond laser imaging device. The laser class 1M, medical IIa device *DermaInspect was* based on a tunable 80 MHz femtosecond titanium:sapphire laser (700–900 nm) and a time-correlated single photon counting (TCSPC) module placed on an optical table. It was also the first certified medical device for fluorescence lifetime imaging (FLIM) [3].

In 2011, a movable multiphoton tomograph (MPT*flex*; Figure 1(b)) with a 360° imaging head mounted on a mechanical arm and an optical arm was introduced. This CE0118-certified medical device enables the examination of human skin in multiple regions of interest including the face or the breast in a comfortable manner. The tomograph with chiller has a total weight of more than 250 kg. The MPT image acquisition is based on the non-linear interaction of near infrared (NIR) 80 MHz femtosecond laser pulses with intracellular intratissue fluorophores and tissue structures. In particular, two major sources of intrinsic image contrast can be utilized: (i) AF and (ii) SHG. In human skin, AF signals are produced from reduced pyridine nucleotides (NADH and NADPH), keratin, flavins/flavoproteins, and melanin in the epidermal layer as well as elastin fibers in the dermis. These biomolecules act as endogenous sources of contrast, avoiding the need for tissue labeling. Additionally, FLIM of the fluorescent metabolic co-factors enables optical metabolic imaging (OMI). SHG signals, generated at exactly half of the excitation wavelength, are in skin exclusively produced from collagen fibers, allowing a clear visualization and

*Corresponding author: Karsten König, Department of Biophotonics and Laser Technology, Saarland University and JenLab GmbH, Germany. Email: k.koenig@blt.uni-saarland.de

Figure 1
Clinical multiphoton tomographs. The certified tomographs *DermaInspect* (a), MPT*flex* (b), and MPT*flex-CARS* (c) are based on a tunable titanium:sapphire laser. The femtosecond laser pulses are guided through an articulated optical mirror arm with beam position sensor and beam correction actuator

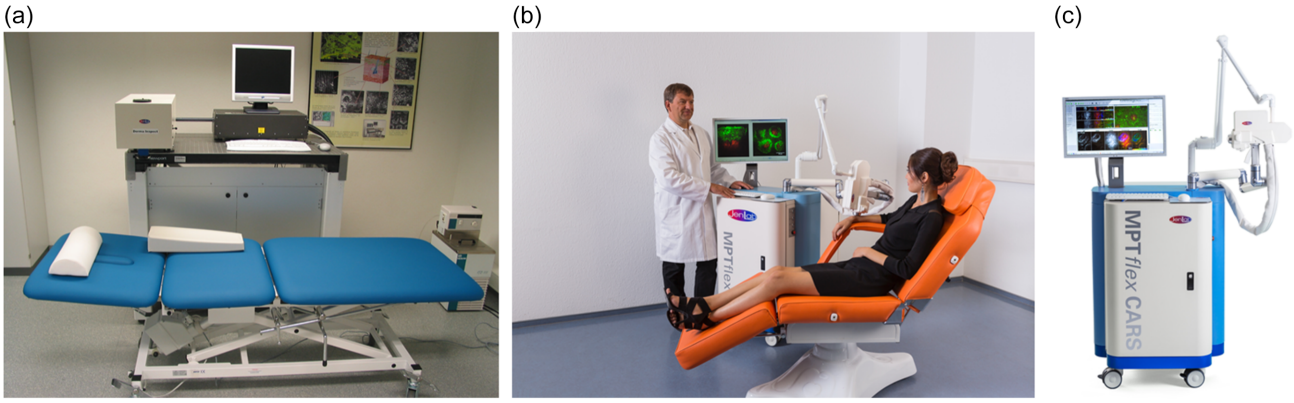

identification of these non-centrosymmetric extracellular matrix structures. Using focusing optics with a high numerical aperture of 1.3, MPT provides the best image resolution (<0.5 µm laterally and 1–2 µm axially) of all clinical imaging methods.

Further improvements of clinical MPT devices included the additional implementation of further multimodality. With the introduction of the two-beam multiphoton tomograph MPT*flex-CARS* (Figure 1(c)), imaging of intratissue lipids was performed in addition to AF, FLIM, and SHG imaging, using an add-on coherent anti-Stokes Raman spectroscopy (CARS) module.

The feasibility and the advantages of the currently available CE-certified medical MPT devices and further two-photon skin imaging microscopes for characterizing the human skin *in vivo* both in medical and cosmetic fields have been largely demonstrated in the past years [3–18]. Its clinical applications include the early detection of malignant melanoma and non-melanoma skin cancer as well as inflammation deceases. Its application in the cosmetic field includes the determination of the efficiency of anti-aging cream and of sunscreen nanoparticle localization.

Current clinical devices for MPT are based on an 80 MHz mode-locked titanium:sapphire laser with tuning ranges between 720 nm and 910 nm and output pulse widths on the order of 100 fs. Typically, these lasers have a large size, a high price, and require water-cooling. This inevitably influences the cost and overall size of MPT devices.

Nevertheless, ultracompact and air-cooled high-power NIR MHz femtosecond laser are now available. In this paper, we describe the implementation of a 50 MHz/80 MHz fiber laser operating at 780 nm into the novel tomograph MPT*compact* and highlight its multimodality. In particular, the NIR femtosecond laser pulses have been also used to realize reflectance confocal microscopy (RCM). Current commercial RCM systems employ a cw laser diode operating at 830 nm with a maximum power around 20 mW [19–21].

The system MPT*compact* with its multimodal possibilities has been tested at the Heidelberg University Hospital and the SRH Wald-Klinikum Gera in the multicenter clinical study EUDAMED No: CIV-18-02-022924 on the normal and diseased human skin *in vivo*. About 100 patients with suspicious, potentially malignant, and pigmented skin lesions have been successfully imaged [22]. A further clinical study is currently conducted at the Massachusetts General Hospital in Boston.

2. Materials and Methods

The fiber laser multiphoton tomograph MPT*compact* is shown in Figure 2. The tomograph is much smaller in size and weight (125 kg) and requires less electromechanical components and less energy consumption. A water chiller is no longer required. The tomograph is based on a passively mode-locked erbium-doped fiber laser with a semiconductor saturable absorber. The air-chilled "Carmel Fiber Based Femtosecond Pulse Laser CFL X-series from CALMAR LASER (Palo Alto, CA)" laser generates sub100-femtosecond pulses with a repetition rate of either 50 MHz or 80 MHz and a maximum laser output power of more than 500 mW. The power consumption is 235 W during measurement and therefore, a factor of 4 less than the tomograph MPT*flex* (0.9 kW–1.1 kW).

The laser output spectrum is also depicted in Figure 2. The laser has a central wavelength of 783 nm with a full width half maximum of 8 nm and a pulse width of about 85 fs, respectively. In addition, a 3.5 smaller shoulder with a maximum at 773 nm occurs. The beam diameter at exit is 1.4 mm, the beam quality $M^2 = 1.1$, and the power stability over 8 h 0.9%. Air-cooling is realized with a low noise fan.

The ultracompact laser head (18 cm × 9 cm × 3.5 cm = 567 cm^3) is directly integrated into the 360° imaging head. A robust armored cable interface connects the laser head within the imaging head with the laser controller module (44 cm × 48 cm × 9.8 cm = 20,700 cm^3) mounted to the medical cart. The integration of the laser head makes the optical mirror arm as employed in the MPT*flex* obsolete. The air-cooled femtosecond fiber laser is significantly smaller than the water-cooled titanium: sapphire lasers MaiTai from Spectra Physics, MKS Instruments, Milpitas, CA (laser head: 61 cm × 35 cm × 15 cm = 32,000 cm^3) and Chameleon from Coherent, Santa Clara, CA (laser head: 61 cm × 37 cm × 19 cm = 43,000 cm^3).

The MPT*compact* device consists of (i) the medical cart, (ii) the laser controller module, (iii) the medical PC with monitor, and (iv) the medical mechanical arm with the 360° imaging head and cable tube. The medical cart is height-adjustable and possesses the two storage batteries, keyboard, mouse, trackball, and the system controller. The system controller operates the safety shutter, the position actuators, the beam attenuator, the galvo scanner, and the photon detectors. The laser controller module on the back side of the medical cart provides the power supply and optical key elements for the laser as well as the RCM photon detector. The medical PC with monitor is based on a 64 bit Windows operating

Figure 2

Photograph, scheme of the optical path, and laser output spectrum of the chiller-free multiphoton tomograph MPT*compact*. The 360° imaging head with scanner, photodetectors, and NA1.3 focusing optics also contains the fiber laser head. The RCM detector detects the back reflection/scattering of the femtosecond laser radiation at 780 nm. The back reflection/scattering is directed back onto the scanner and then focused onto the facet of an optical fiber. The optical fiber acts as pinhole

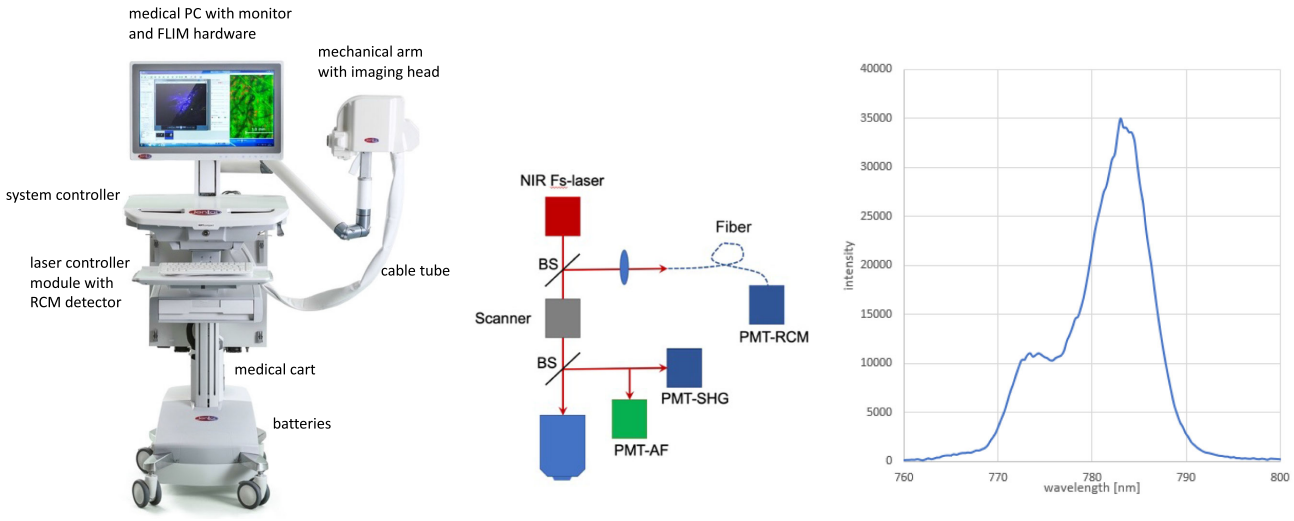

Note: BS: beam splitter, PMT: photomultiplier tube

system (ZEUS, Onyx Healthcare Inc., New Taipei City). The computer contains the *JenLab* Scan software, the *JenLab* Image software, JenLab's "White Light Imager" software, the FLIM TimeHarp *260* hardware (PCI interface), and data acquisition software "SymPhoTime 64"/"PTUCutter" (Picoquant, Berlin, Germany), as well as the laser control software.

The medical mechanical arm has a locking mechanism to fix the imaging head on the target and to avoid major motion artifacts. The 360° imaging head can be used in any direction, in particular, as inverted or upright optical system. It contains the ultracompact laser head, x/y/z actuators, the galvo scanner, NA1.3 focusing optics, a beam expander and beam attenuator, two fast photomultipliers for TCSPC for AF imaging and SHG imaging, a safety shutter, a LED module with camera called "White Light Imager," and parts of the RCM module. Furthermore, it contains a motorized x,y stage (blue stage) that can "move" the tissue within a 40 × 40 mm^2 area.

The "White Light Imager" provides 800 px × 800 px images based on the illumination with 4 LEDs (100 lm, 100 ms flashlight) and a CMOS sensor providing a 1.83 MB bmp file with 24 bit color depth. Autocorrection takes place to correct for distortion effects due to the 45° observation angle. During white light imaging, the focusing optics is automatically moved away in order not to influence the 10 × 10 mm^2 wide field image.

The RCM module detects the reflected/backscattered photons of the femtosecond laser radiation at 780 nm. These photons are directed through the NA1.3 focusing optics back onto the galvo scanner and then focused onto the facet of an optical fiber. The glass fiber acts as pinhole. The fiber transmits the photons to the RCM photon detector.

Two-photon excited AF signals and SHG signals are detected with miniaturized TCSPC photomultipliers without transmission through the galvo scanner. Parallel acquisition of AF, SHG as well as RCM signals with its three photon detectors turns the MPT*compact* in a multimodal imaging device with 250 ps temporal resolution.

The lateral resolution was determined by imaging green-fluorescent nanobeads with a diameter of 100 nm. The point spread function of the fluorescence signal revealed an excellent lateral resolution of 0.3 µm and an axial resolution of about 2 µm. This high spatial resolution based on the high-NA oil objective allows imaging of single elastin fibers and single intratissue mitochondria.

The high NA value was chosen according to safety regulations of the former CE0118-certified multiphoton tomographs for human skin imaging. According to these regulations, also a maximum mean power of 50 mW at the skin must be considered.

The maximum imaging depth is determined by the working distance of the focusing optics that is 200 µm in combination with a 160 µm thick cover slip.

The step motor-driven focusing optics in combination with the galvo scanner and the motorized stage is used (i) to realize automated optical sectioning, (ii) to search for region of interest (ROIs) in a target field of 4 × 4 mm^2, as well as (iii) to perform large-field multiphoton imaging by stitching (mosaic: several scan fields next to each other).

The system is freely movable. It even contains onboard storage batteries so that it can operate for up to a few hours independently from external power supply.

The magnetic "MPT interface" between the blue motorized stage of the 360° imaging head and the tissue consists of a metallic ring (diameter of 41 mm) with a round 160 µm thick cover slip that is taped onto the skin (Figure 3).

3. Results

The multimodal tomograph MPT*compact* has five imaging modalities. In particular, it provides simultaneously high-resolution (submicron) (i) AF images, (ii) SHG images, and (iii) confocal reflectance microscopy (CRM) images. Furthermore, FLIM images can be generated based on TCSPC with picosecond temporal resolution and biexponential fitting. In that case, the false color represents either the mean fluorescence lifetime, the lifetime of the short-lived component, or the component with the long fluorescence lifetime. This enables OMI when

Figure 3

MPT interface. The NA1.3 focusing optics of the multiphoton tomograph has no direct contact to the skin. A metal ring with a 0.16 mm thick round coverslip is taped to the skin. A drop of oil immersion is applied to the top of the coverslip and a drop of PBS/water beneath the coverslip. The MPT interface is magnetically connected to the blue-motorized stage of the 360° imaging head

imaging the fluorescence decay of the coenzymes NAD(P)H and flavins. The fifth imaging modality is "dermoscopy" with the LED light and camera. Before starting the MPT measurements, the "MPT interface" between the high NA1.3 focusing optics of the tomograph and the skin needs to be taped to the skin. Afterwards, a white light image with the internal LED illumination source and the camera can be taken through the 160 µm thick glass window of the interface. The white light image with a field of view (FOV) of 10 × 10 mm^2 can be used for the imaging of the suspicious skin lesion and for the determination of a ROI for MPT (Figure 4). It can also be used to perform dermoscopy.

After choosing the ROI, the RCM module of the tomograph MPT*compact* can be used for rapid skin screening because the high number of reflected/scattered femtosecond laser photons can be employed to realize a scanning speed of one frame per second or faster. Also a very fast line scanning mode can be employed. The RCM mode enables to find very fast the skin's surface and a ROI of interest and, therefore, helps to reduce the MPT examination time. Different skin positions can be screened using the trackball for moving fast in all three directions by the motorized blue stage and the motor-driven focusing optics.

Figure 4

White light image of a suspicious pigmented skin lesion. The image taken with LED excitation and a CMOS camera has a field of view of 10 × 10 mm^2. The blue rectangles are regions of interests that have been investigated by optical multiphoton sectioning with a FOV of 0.3 × 0.3 mm^2

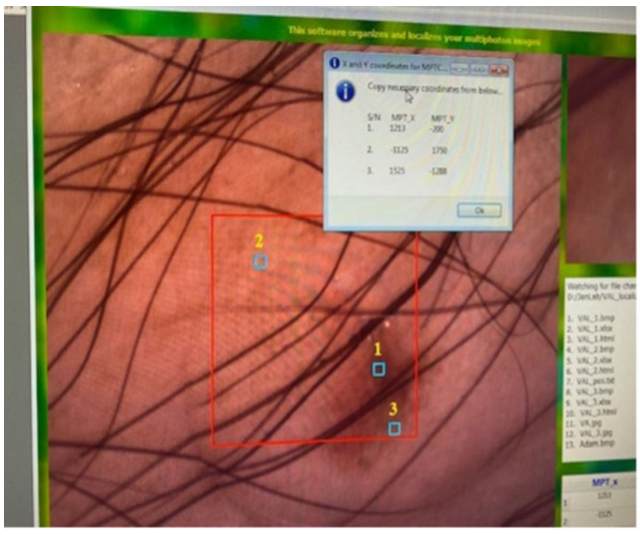

Afterwards, the scan speed is typically set to 4–6 s per frame in order to obtain high contrast AF, FLIM, SHG, and RCM images without the need of averaging. All photon signals are recorded simultaneously. Six images can be displayed on the screen, three of them "digital" with the numbers of photons counted on each pixel. The other three "analog" channels contain grey values (16 bit/32 bit). The AF, SHG, and RCM images are depicted line-by-line in "real time". In addition, a colored overlay image of the three signals can be generated (Figure 5).

Typically, a mean power of 20 mW is chosen to perform optical sectioning. The power can be also increased stepwise up to a maximum value of 50 mW, when going deep. Typically, stacks of 21 horizontal images ("en face") in 10 µm steps are generated to cover the skin layers from the surface (stratum corneum) down through the epidermal layers stratum granulosum, stratum spinosum, and stratum basale to the papillary dermis in maximum 0.2 mm depth (working distance of the focusing optics). The depth, where the onset of the SHG signal generated by collagen starts, indicates the thickness of the epidermis.

The typical frame size is 0.3 × 0.3 mm^2 (512 × 512 pixels, 40× focusing optics). An optical zoom and an electronic zoom can be used to highlight intracellular structures, e.g., to visualize single autofluorescent mitochondria or clusters of nanoparticles in a FOV, e.g., 100 × 100 $µm^2$. The step width can also be reduced to a value of 0.5 µm. In addition, vertical sectioning can be performed ("x,z sections").

When obtaining multiphoton features of interest, the examiner can choose to investigate neighboring skin areas. Nine neighboring stacks would cover about 1 mm^2 and can be realized with the motorized stage ("mosaicing") within 10 min (6 s per section, 1 min for 10 sections) or less than 2 min (1 s per section). FLIM does not require extra time for acquisition. However, biexponential decay fitting and the generation of false color images may require an additional minute calculation time per frame.

In order to optimize the multiphoton investigation, e.g. to take images without the presence of a strong fluorescent hair in the images, (i) the beam position can be varied using the x/y-position window or (ii) the trackball can be used.

"Fast FLIM" images can be rapidly calculated and shown on-line ("in real time") during scanning (Figure 6). Furthermore, high-contrast FLIM images can be generated after measurement from the raw AF data after biexponential least-squares fitting (multi-exponential fitting up to 5 exponentials theoretically possible) of the fluorescence decay curves per pixel. A short fluorescence lifetime

Figure 5

Screenshot of the monitor's screen during operation. A stack of AF/SHG/RCM optical sections is taken. The upper black and white analog images as well as the colored image as overlay of the three signals are monitored "on-line" with a frame rate of 6 s. The left side shows the recording mode, the x,y,z-beam position, the zoom, the mean power value, and its possible modification with tissue depth. The right side depicts PMT parameters and positions of the stage

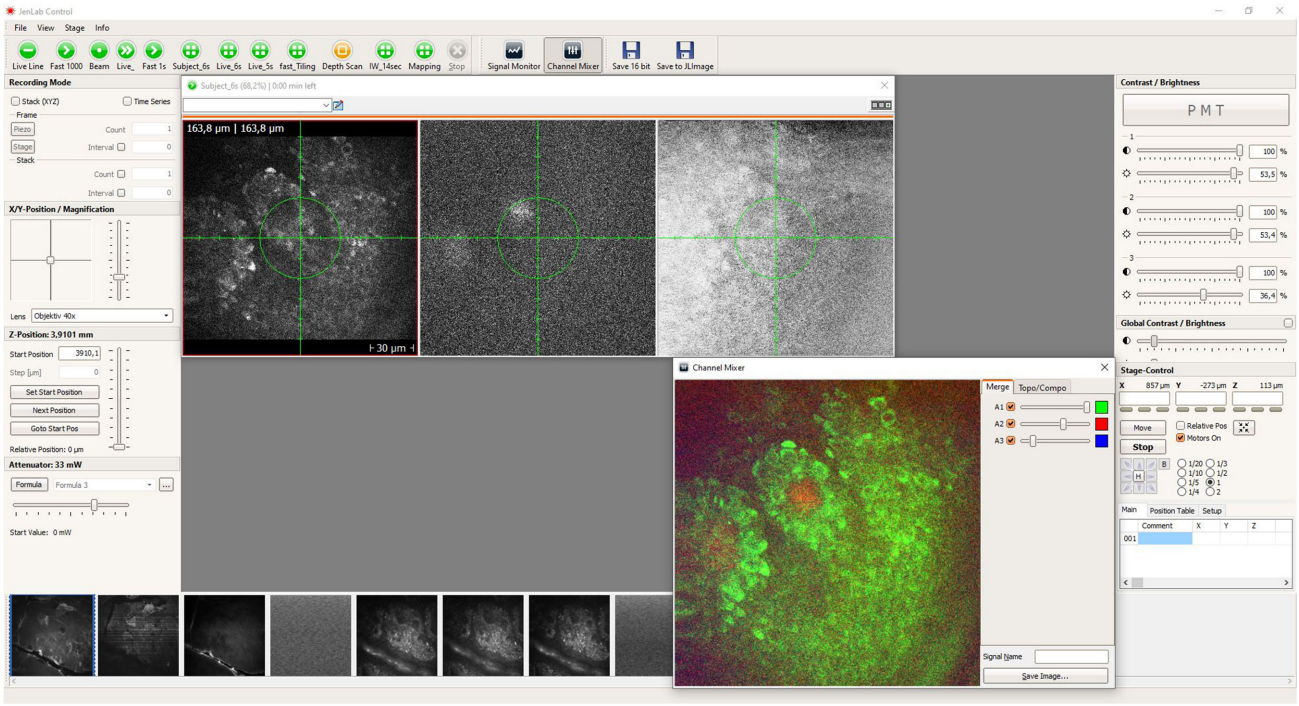

Figure 6

"Fast FLIM" image. This pseudo-colored FLIM image can be seen on-line during scanning due to fast data processing

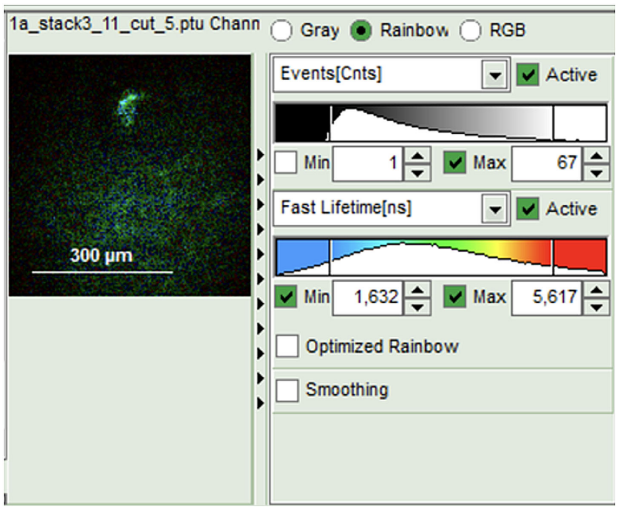

component in the sub-nanosecond range (e.g. "free NADH" component), a long-lived component of about 2 ns (e.g. "protein-bound NADH component"), and the mean fluorescence lifetime, e.g., of about 1, ns can be depicted in false colors.

Figure 7 shows images of the forearm skin of a healthy volunteer at two tissue depths (stratum spinosum and the epidermal–dermal junction) obtained with 5 imaging modalities to demonstrate the potential of this novel multimodal tomograph. The white light camera image provides an overall view of the imaging area.

AF, SHG, and RCM optical sections have been recorded simultaneously. The FLIM image was generated after the stack measurement within 2 min.

Based on the tissue AF, the cell's architecture (fluorescent mitochondria and cytoplasm, nonfluorescent nucleus) and elastin fibers are depicted. The RCM image provides additional contrast due to backscattered light from structures like cell membranes and melanosomes. Additionally, the pseudo-colored FLIM image from the AF decay curves per pixel is shown. FLIM provides information on cellular metabolism, in particular, when measuring the ratio of free to bound NADH (free NADH has an AF lifetime of about 0.3 ns, bound NADH of about 2 ns) as an OMI indicator. With SHG imaging, information on the dermal collagen fibers and the thickness of the epidermal layer can be retrieved.

4. Discussion

The third generation of commercial multiphoton tomographs (MPT*compact*) provides enhanced compactness and portability, less energy consumption, and multimodality at a lower price. The tomograph is based on an erbium-doped femtosecond fiber laser and miniaturized multiple detectors to realize multimodality by simultaneous optical sectioning including one-photon confocal imaging.

The use of the ultracompact air-cooled fiber laser (560 cm^3) compared to the conventional water-cooled tunable titanium:

Figure 7

Multimodal imaging with the fiber laser tomograph MPT*compact*. The figure shows representative images of human skin *in vivo* from two depths employing two-photon excited AF, SHG of collagen fibers, RCM, and their overlay (green – AF; red – SHG; blue – RCM). Additionally, the autofluorescence lifetime image and a white light CCD image with a magnified view of the skin area are also shown

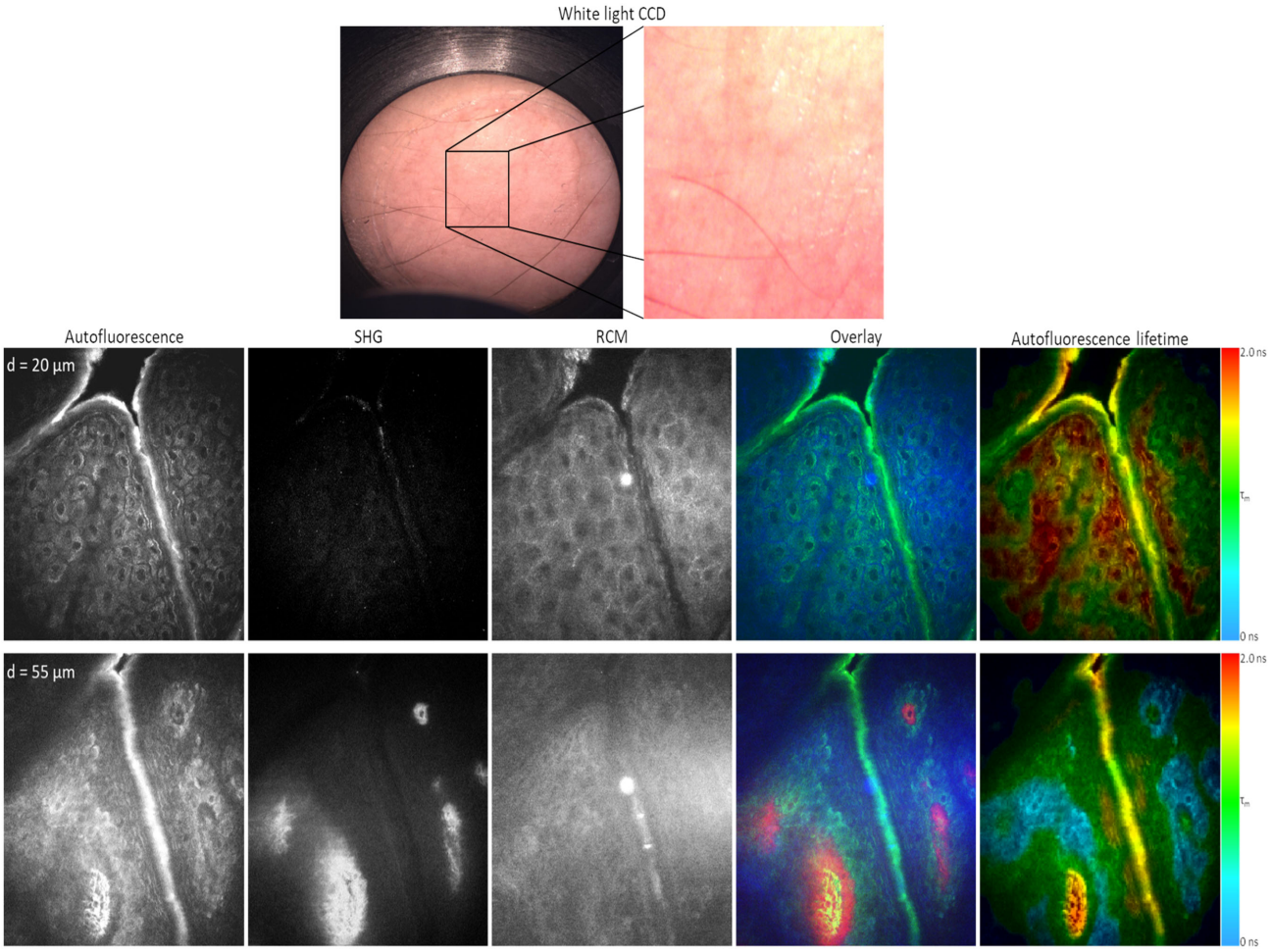

sapphire laser reduces the weight by a factor of 2 and the energy consumption by a factor of 4. The laser head is integrated in the imaging head. This design eliminates the use of the optical articulated arm with active beam alignment by a motorized mirror as realized in the tomographs "*DermaInspect*" and "MPT*flex*".

With the multimodal multiphoton tomograph MPT*compact*, rapid label-free in vivo histology with subcellular resolution can be performed within minutes based on AF, SHG, FLIM, RCM, and dermoscopy.

Most useful information is provided by the two-photon excited intratissue AF of the coenzymes NAD(P)H and flavins. The fluorescence of these coenzymes and the high lateral resolution of 0.3 µm enables the visualization of single intratissue mitochondria as well as the cytoplasm. Interestingly, both coenzymes can be excited at a laser wavelength of 780 nm. Therefore, tunable femtosecond lasers such as the MaiTai or the Chameleon are not explicitly required for two-photon coenzyme imaging.

The signals of both types of coenzymes (NAD(P)H and flavins/ flavoproteins) can be separated by FLIM. Furthermore, the free and protein-bound form can be distinguished by time-resolved AF detection with picosecond temporal resolution. For example, protein-bound NADH has one order higher AF lifetime than free (non-bound) NADH. Label-free OMI based on two-photon FLIM is also a perfect method to gain information on the cell's metabolism. Both the ratio of NAD(P)H to flavins and the ratio free to bound NAD(P)H based on FLIM data (amplitudes of short-lived and long-lived components) can be used as parameters to investigate metabolic changes.

The laser wavelength of 780 nm is also suitable to image intratissue melanin. In fact, less laser power is required to detect melanin compared with NAD(P) and flavins. It is therefore easy to image intratissue human hair and to investigate pigmented lesions. Of special interest is the detection of early signs of malignant melanoma. One important feature of MPT is the detection of melanocytes due to the two-photon excited AF of melanin. Interestingly, the dendrites of melanocytes can be imaged due to the presence of melanin in the spines. By optical sectioning, migrating melanocytes in the case of malignant melanoma can be imaged in the upper epidermis and upper dermis. The mean AF lifetime of melanin is much shorter than the mean lifetimes of NAD(P)H and flavins. Therefore, FLIM provides another contrast imaging method to depict melanin in the optical biopsy.

The most useful information of second harmonic imaging (SHG) of human skin is the image of the collagen network. The SHG signal occurs at a wavelength of 390 nm. The SHG signal is generated in forward direction but effectively back reflected to a large degree due to scattering. However, due to multiple scattering, a large amount of the SHG photons is backscattered and can be detected by the SHG photomultiplier.

Based on the skin type, SHG imaging down to a depth of 150 µm and deeper to 200 µm is possible. Typically, the onset of SHG signals in a human arm occurs at depths between 50 µm and 70 µm. In fact, when going deep by optical sectioning, the first SHG signals define the epidermal–dermal junction. The accuracy to determine the epidermal thickness based on SHG images is given by the axial resolution of 2–3 µm. SHG imaging is also used to determine the skin age parameter SAAID that is defined as ratio of elastin signal to collagen signal [9]. The elastin signal is based on AF. The calculation of the skin age parameter based on MPT imaging is used by the leading cosmetic companies to verify anti-aging effects by their products. Also the SAAID values of five astronauts have been determined by MPT to evaluate the effects of long-term space flights on skin [9].

For the first time, NIR femtosecond laser pulses have been used to realize reflectance confocal imaging (RCM) of human skin. The backscattered/reflected photons have been transmitted through an optical fiber that acts simultaneously as pinhole due to the small micrometer-sized diameter. The detector is placed on the distal part of the fiber and can therefore be positioned outside the imaging head. The multimodal tomograph provides high-resolution RCM images. In fact, the submicron lateral resolution is higher than today's commercial RCM devices for dermatology and ophthalmology due to the use of focusing optics with the very high numerical aperture of 1.3 and the shorter laser wavelength of 780 nm compared to 830 nm. The RCM images provides the additional information of the location of cell membranes. Both RCM and two-photon AF imaging can visualize melanin.

The tomograph MPT*compact* has been successfully tested in a clinical multicenter study for the diagnosis of malignant melanoma on 100 patients with suspicious pigmented lesions with the goal to improve the diagnosis of early malignant melanoma [11, 18].

The digital images contain the number of detected photons per pixel and their arrival times. This information can be used to realize quantitative imaging, e.g., to generate FLIM images [4], the skin aging index SAAID, and molecular concentrations maps after calibration. The data can be also employed for image processing with artificial intelligence/neuronal networks, e.g., to identify melanocytes with their fluorescent spines in the upper epidermis and upper dermis as one major indicator in the diagnosis of malignant melanoma [22, 23].

Still the doctor has to find a suspicious skin lesion and has to define a ROI by white field imaging or the naked eye. A first confocal RCM screening can be performed to get additional information from inside the skin. Widefield and RCM images can only show the basic structural information of human skin based on reflected/backscattered photons. MPT stacks provide additional information on the extracellular network and the cell's metabolism. In principle, skin areas may appear structurally normal but can be identified as lesions with MPT.

As in the case of an invasive physically taken biopsy combined with conventional histology that is based on the doctor's examination with the dermatoscope or the naked eye, deep skin lesions can be overseen. However, more important is the fact that MPT has the potential to reduce the number of physically taken skin biopsies.

5. Conclusions

The compact and flexible design of the multiphoton tomograph MPT*compact* combined with its affordable price facilitate its introduction into clinic practice to support the dermatologist to diagnose different skin pathologies and to reduce the number of physically taken biopsies.

For the first time, multiphoton tomographs provide an additional module for high-resolution CRM. CRM is already used in the dermatological practice for the diagnosis of non-melanoma cancer [19]. The main three MPT signals (i) two-photon AF, (ii) SHG, and (iii) two-photon FLIM provide even much better histological information and important metabolic information than CRM signals. Because the tomograph MPT*compact* combines two-photon imaging and CRM, this novel skin imaging tool has the potential to enhance patient care and streamline medical procedures, including MPT-guided surgery.

Furthermore, its application within the cosmetic and pharmaceutical industries holds promise for advancing our understanding of anti-aging treatments and pharmaceuticals, ultimately leading to more effective products and reducing the reliance number on animal testing.

Future potential applications include monitoring the impact of climate change such as "dry skin" by environmental shifts and assessing the effects of air pollution on skin health, particularly in cases of chronic inflammation due to nanoparticle exposure. The tomograph MPT*compact* operates with batteries and can be sun-powered, which helps to perform skin measurements even in remote and harsh environment. MPT can be used to study how our environment affects our skin, opening up new avenues for research, prevention, and personalized healthcare.

The multiphoton tomograph represents a remarkable fusion of science, technology, and medicine and may hopefully will make profound contributions to both clinical practice and scientific discoveries.

Funding Support

The author acknowledges financial support from the European Union under the HORIZON 2020 SME project LASER-HISTO (Grant Agreement No: 726666).

Ethical Statement

This study does not contain any studies with human or animal subjects performed by the author.

Conflicts of Interest

The author declares that he has no conflicts of interest to this work. The author is the founder and CEO of the company JenLab GmbH.

Data Availability Statement

Data sharing is not applicable to this article as no new data were created or analyzed in this paper. The data including the final report that supports the findings of the multicenter multiphoton skin imaging study "Mi-MulTo" are available in the *European Database of Medical Devices (EUDAMED)* and the *German Medical Device Information and DATA Bank System (DIMDI)* of the *Bundesinstitut für Arzneimittel und Medizinprodukte (BfArM)* under the EUDAMED number CIV-18-02-022924 at www.bfarm.de and in reference [22].

Institutional Review Board Statement

The clinical multicenter study was conducted in accordance with the Declaration of Helsinki and approved by the Ethics Commission (registration number: DE/EKTH47/00011267).

Informed Consent Statement

Written informed consent has been obtained from the patients to perform the multicenter study.

References

[1] Denk, W., Strickler, J. H., & Webb, W. W. (1990). Two-photon laser scanning fluorescence microscopy. *Science*, *248*(4951), 73–76. https://doi.org/10.1126/science.2321027

[2] König, K. (2023). Medical femtosecond laser. *Journal of the European Optical Society-Rapid Publications*, *19*(2), 36.

[3] Fischer, F. F., Volkmer, B., Puschmann, S., Greinert, R., Breitbart, W., Kiefer, J., & Wepf, R. (2008). Risk estimation of skin damage due to ultrashort pulsed, focused near-infrared laser irradiation at 800 nm. *Journal of Biomedical Optics*, *13*(4), 041320. https://doi.org/10.1117/1.2960016

[4] Becker, W., Bergmann, A., Ibarrola, R. S., Müller, P. F., & Braun, L. (2019). Metabolic imaging by simultaneous FLIM of NAD (P) H and FAD. In *Multiphoton Microscopy in the Biomedical Sciences XIX, 10882*, 108820B. https://doi.org/10.1117/12.2510132

[5] Borile, G., Sandrin, D., Filippi, A., Anderson, K. I., & Romanato, F. (2021). Label-free multiphoton microscopy: Much more than fancy images. *International Journal of Molecular Sciences*, *22*(5), 2657. https://doi.org/10.3390/ijms22052657

[6] Dancik, Y., Favre, A., Loy, C. J., Zvyagin, A. V., & Roberts, M. S. (2013). Use of multiphoton tomography and fluorescence lifetime imaging to investigate skin pigmentation in vivo. *Journal of Biomedical Optics*, *18*(2), 026022. https://doi.org/10.1117/1.JBO.18.2.026022

[7] Georgakoudi, I., & Quinn, K. P. (2023). Label-free optical metabolic imaging in cells and tissues. *Annual Review of Biomedical Engineering*, *25*, 413–443. https://doi.org/10.1146/annurev-bioeng-071516-044730

[8] Fast, A., Lal, A., Durkin, A. F., Lentsch, G., Harris, R. M., Zachary, C. B., . . . , & Balu, M. (2020). Fast, large area multiphoton exoscope (FLAME) for macroscopic imaging with microscopic resolution of human skin. *Scientific Reports*, *10*(1), 18093. https://doi.org/10.1038/s41598-020-75172-9

[9] König, K. (2018). Multiphoton tomography (MPT). In K. König (Ed.), *Multiphoton microscopy and fluorescence lifetime imaging: Applications in biology and medicine* (pp. 247–268). Germany: De Gruyter. https://doi.org/10.1515/9783110429985-015

[10] Li, J., Wilson, M. N., Bower, A. J., Marjanovic, M., Chaney, E. J., Barkalifa, R., & Boppart, S. A. (2020). Video-rate multimodal multiphoton imaging and three-dimensional characterization of cellular dynamics in wounded skin. *Journal of Innovative Optical Health Sciences*, *13*(2), 2050007. https://doi.org/10.1142/S1793545820500078

[11] Pena, A. M., Ito, S., Bornschlögl, T., Brizion, S., Wakamatsu, K., & Del Bino, S. (2023). Multiphoton FLIM analyses of native and UVA-modified synthetic melanins. *International Journal of Molecular Sciences*, *24*(5), 4517. https://doi.org/10.3390/ijms24054517

[12] Pittet, J. C., Freis, O., Vazquez-Duchêne, M. D., Périé, G., & Pauly, G. (2014). Evaluation of elastin/collagen content in human dermis in-vivo by multiphoton tomography—Variation with depth and correlation with aging. *Cosmetics*, *1*(3), 211–221. https://doi.org/10.3390/cosmetics1030211

[13] Pouli, D., Balu, M., Alonzo, C. A., Liu, Z., Quinn, K. P., Rius-Diaz, F., . . . , & Georgakoudi, I. (2016). Imaging mitochondrial dynamics in human skin reveals depth-dependent hypoxia and malignant potential for diagnosis. *Science Translational Medicine*, *8*(367), 367ra169. https://doi.org/10.1126/scitranslmed.aag2202

[14] Puschmann, S., Rahn, C. D., Wenck, H., Gallinat, S., & Fischer, F. F. (2012). Approach to quantify human dermal skin aging using multiphoton laser scanning microscopy. *Journal of Biomedical Optics*, *17*(3), 036005. https://doi.org/10.1117/1.JBO.17.3.036005

[15] Sugata, K., Osanai, O., Sano, T., & Takema, Y. (2011). Evaluation of photoaging in facial skin by multiphoton laser scanning microscopy. *Skin Research & Technology*, *17*(1), 1–3. https://doi.org/10.1111/j.1600-0846.2010.00475.x

[16] Tancrède-Bohin, E., Baldeweck, T., Brizion, S., Decencière, E., Victorin, S., Ngo, B., . . . , & Pena, A. M. (2020). In vivo multiphoton imaging for non-invasive time course assessment of retinoids effects on human skin. *Skin Research & Technology*, *26*(6), 794–803. https://doi.org/10.1111/srt.12877

[17] Yew, E., Rowlands, C., & So, P. T. C. (2014). Application of multiphoton microscopy in dermatological studies: A mini-review. *Journal of Innovative Optical Health Sciences*, *7*(5), 1330010. https://doi.org/10.1142/S1793545813300103

[18] Zhao, J., Zhao, Y., Wu, Z., Tian, Y., & Zeng, H. (2023). Nonlinear optical microscopy for skin in vivo: Basics, development and applications. *Journal of Innovative Optical Health Sciences*, *16*(1), 2230018. https://doi.org/10.1142/S179354582230018X

[19] Braghiroli, N. F., Sugerik, S., Freitas, L. A. R. D., Oliviero, M., & Rabinovitz, H. (2022). The skin through reflectance confocal microscopy-Historical background, technical principles, and its correlation with histopathology. *Anais Brasileiros de Dermatologia*, *97*(6), 697–703. https://doi.org/10.1016/j.abd.2021.10.010

[20] Calzavara-Pinton, P., Longo, C., Venturini, M., Sala, R., & Pellacani, G. (2008). Reflectance confocal microscopy for in vivo skin imaging. *Photochemistry and Photobiology*, *84*(6), 1421–1430. https://doi.org/10.1111/j.1751-1097.2008.00443.x

[21] Lboukili, I., Stamatas, G., & Descombes, X. (2022). Automating reflectance confocal microscopy image analysis for dermatological research: A review. *Journal of Biomedical Optics*, *27*(7), 070902. https://doi.org/10.1117/1.JBO.27.7.070902

[22] König, K., Pankin, D., Paudel, A., Hänßle, H., Winkler, J. K., Zieger, M., & Kaatz, M. (2021). Skin cancer detection with a compact multimodal fiber laser multiphoton FLIM tomograph. In *Multiphoton Microscopy in the Biomedical Sciences XXI, 11648*, 116480A. https://doi.org/10.1117/12.2577608

[23] Haggenmüller, S., Maron, R. C., Hekler, A., Utikal, J. S., Barata, C., Barnhill, R. L., . . . , & Brinker, T. J. (2021). Skin cancer classification via convolutional neural networks: Systematic review of studies involving human experts. *European Journal of Cancer*, *156*, 202–216. https://doi.org/10.1016/j.ejca.2021.06.049

How to Cite: König, K. (2024). Multimodal Multiphoton Tomography with a Compact Femtosecond Fiber Laser. *Journal of Optics and Photonics Research*, *1*(2), 51–58. https://doi.org/10.47852/bonviewJOPR32021730